



# Hyperglycemia-Driven Neuroinflammation Compromises BBB Leading to Memory Loss in Both Diabetes Mellitus (DM) Type 1 and Type 2 Mouse Models

Slava Rom<sup>1,2</sup> · Viviana Zuluaga-Ramirez<sup>1</sup> · Sachin Gajghate<sup>1</sup> · Alecia Seliga<sup>1</sup> · Malika Winfield<sup>1</sup> · Nathan A. Heldt<sup>1</sup> · Mikhail A. Kolpakov<sup>3</sup> · Yulia V. Bashkirova<sup>3</sup> · Abdel Karim Sabri<sup>3</sup> · Yuri Persidsky<sup>1,2</sup>

Received: 28 February 2018 / Accepted: 26 June 2018 / Published online: 5 July 2018  
© Springer Science+Business Media, LLC, part of Springer Nature 2018

## Abstract

End organ injury in diabetes mellitus (DM) is driven by microvascular compromise (including diabetic retinopathy and nephropathy). Cognitive impairment is a well-known complication of DM types 1 and 2; however, its mechanism(s) is(are) not known. We hypothesized that blood-brain barrier (BBB) compromise plays a key role in cognitive decline in DM. Using a DM type 1 model (streptozotocin injected C57BL/6 mice) and type 2 model (leptin knockout obese db/db mice), we showed enhanced BBB permeability and memory loss (Y maze, water maze) that are associated with hyperglycemia. Gene profiling in isolated microvessels from DM type 1 animals demonstrated deregulated expression of 54 genes related to angiogenesis, inflammation, vasoconstriction/vasodilation, and platelet activation pathways by at least 2-fold (including eNOS, TNF $\alpha$ , TGF $\beta$ 1, VCAM-1, E-selectin, several chemokines, and MMP9). Further, the magnitude of gene expression was linked to degree of cognitive decline in DM type 1 animals. Gene analysis in brain microvessels of DM type 2 db/db animals showed alterations of similar genes as in DM 1 model, some to an even greater extent. Neuropathologic analyses of brain tissue derived from DM mice showed microglial activation, expression of ICAM-1, and attenuated coverage of pericytes compared to controls. There was a significant upregulation of inflammatory genes in brain tissue in both DM models. Taken together, our findings indicate that BBB compromise in DM in vivo models and its association with memory deficits, gene alterations in brain endothelium, and neuroinflammation. Prevention of BBB injury may be a new therapeutic approach to prevent cognitive demise in DM.

**Keywords** BBB · Endothelial dysfunction · Diabetes · Dementia · Inflammation

## Introduction

Development of cognitive impairment/dementia and its links to various pathologic conditions remains elusive. A number of underlying mechanisms/causes has been proposed including

genetic defects in Alzheimer's disease (AD) and Parkinson's disease, metabolic dysfunctions (diabetes, homocysteinemia, toxic environmental factors, effects of drugs, etc.), hypertension, chronic neuroinflammatory conditions (autoimmune or infectious origin), and traumatic brain injury. Yet, up to 40% of these conditions converge on defects in the brain microvasculature [1] and its coupling to neuronal functions resulting in hypo-perfusion and eventual neuronal demise [2]. Rapid progress with brain imaging, allowing evaluated perfusion in conjunction with structural changes and neuronal function, speed such studies. Understanding of the mechanisms of such changes is of high significance due to potential of harnessing novel therapeutic interventions. It is fully applicable to cognitive demise in patients suffering from diabetes mellitus (DM) type 1 or type 2 [3–5]. DM is a metabolic disease related to the inability to produce insulin and proper utilization of glucose (type 1) or insulin resistance when this hormone is produced but cannot interact with its receptors (type 2). Both conditions

✉ Slava Rom  
srom@temple.edu

✉ Yuri Persidsky  
yuri.persidsky@tuhs.temple.edu

<sup>1</sup> Department of Pathology and Laboratory Medicine, Lewis Katz School of Medicine, Temple University, Philadelphia, PA 19140, USA

<sup>2</sup> Center for Substance Abuse Research, Lewis Katz School of Medicine, Temple University, Philadelphia, PA 19140, USA

<sup>3</sup> Cardiovascular Research Center, Lewis Katz School of Medicine, Temple University, Philadelphia, PA 19140, USA

result in high glucose levels in blood, enhanced generation of reactive oxygen species (ROS), and end organ injury stemming from microvascular abnormalities [6]. Examples of such well-documented DM complications are cardiovascular disease, nephropathy, and retinopathy, all stemming from microvascular injury. The relationship between microvascular changes and cognitive decline in DM had not been substantiated until very recently, including blood perfusion, neuronal function, white matter microstructure, and metabolic function [7]. Overall small vessel abnormalities documented in DM include white matter lesions, microbleeds, silent brain infarcts, and lacunar abnormalities, indicative of cognitive decline [8].

Besides changes in blood supply, another important factor in DM is increased permeability of the blood-brain barrier (BBB) [9]. The BBB is composed of highly specialized brain microvascular endothelial cells (BMVEC) connected by tight junctions (TJ) with very low pinocytotic activity and uniquely expressed transporters. The function of BMVEC is supported by pericytes enveloping the abluminal side of brain endothelium [10]. Proper function of the BBB ensures protection of the central nervous system (CNS) unique milieu and restricts penetration of toxic substances across the barrier, while providing an adequate supply of nutrients. Disruption of the BBB and its association with cognitive decline has been recently demonstrated in DM patients [11] and was associated with increased levels of vascular dysfunction markers in cerebrospinal fluid (CSF). Indicators of BBB injury have better predictive power for dementia development than genetic hallmarks of AD. Further, memory deficits have been documented in animal models of DM [12], which showed BBB dysfunction [13] paralleling a loss of pericytes and neuronal dysfunction. Causes for vascular dysfunction in DM are related to heightened generation of ROS due to enhanced glucose metabolism, subsequent buildup of glycolytic intermediates, advanced glycation end products (AGEs), and activation of protein kinase C (PKC) [14, 15]. These events eventually may result in NF- $\kappa$ B activation, overexpression of adhesion molecules (VCAM-1, ICAM-1), activation of the small GTPase, RhoA, and diminished expression of TJ proteins [16]. The relationship between glucose levels and cognitive decline is complex. In humans, higher blood glucose levels were associated with worse cognitive performance [17, 18], while a recent report suggested that a history of severe hypoglycemic episodes was associated with a greater risk of dementia [19]. However, the exact mechanisms of injury, differences between DM type 1 and 2, and the therapeutic potential of BBB protective strategies in cognitive decline are currently unknown. Here, we explored the hypothesis that DM types 1 and 2 decrease BBB integrity directly (via effects on brain endothelium and pericytes) and promote a pro-inflammatory phenotype of brain endothelium (resulting in low-level inflammation) that further exacerbates barrier injury. We used animal models of DM types 1 and 2 and showed increased BBB permeabilities that are associated with

hyperglycemia. Importantly, these animals demonstrated cognitive decline paralleling BBB injury. Profiling of genes in CNS microvessels isolated from these animals showed upregulation of pro-inflammatory and barrier destabilizing molecules. The magnitude of their expression interrelated with cognitive abnormalities. Neuroinflammatory responses in both animal models were associated with a decrease of pericyte BBB coverage. Our report provides evidence from animal models for the causes of vascular dementia, and might lead to development of future therapeutics to diminish its burden.

## Materials and Methods

### Animals

C57BL/6 mice (10-week-old male) as well as leptin-deficient mice  $db^{+}/db^{+}$  (further  $db/db$ ) and leptin heterozygous  $db^{+}/db^{-}$  (further  $db/hemi$ ) were acquired from the Jackson Laboratory (Bar Harbor, ME). To achieve statistical significance in each experiment, mice were divided into groups of 6 to 10 animals (exact numbers for each experiment are indicated in figure legends).

All in vivo experiments were approved by the Temple University Institutional Animal Care and Use Committee in accordance with guidelines based on the National Institutes of Health (NIH) guide for care and use of laboratory animals and Animal Research: Reporting In Vivo Experiments (ARRIVE) guidelines ([www.nc3rs.org.uk/arrive-guidelines](http://www.nc3rs.org.uk/arrive-guidelines)).

### Induction of Diabetes

Diabetes type 1 was induced as described [20]. In short, C57BL/6 mice (10 week old, 25–30-g body weight) were randomly divided into groups. One group received once daily intraperitoneal (ip) injection of streptozotocin (STZ) for five consecutive days (50 mg/kg in citrate buffer, pH 4.5, freshly made every day). Control group mice received citrate buffer only. The first day of STZ injection was assigned as the starting time for diabetes. Serum glucose concentrations were monitored on 7 days, 4, 8, and 12 weeks after the start. Blood glucose levels (BGL) were determined by glucose analyzer (Bayer Contour®, Ascensia Diabetes Care, Parsippany, NJ), according to manufacturer's instructions.

### Y Maze Exploratory Memory Test

Spontaneous exploratory behavior was investigated by using a Y maze as described [21–23]. The Y maze apparatus consists of three arms, each 21 cm long, 4 cm wide, and 40 cm tall with a central entry zone. It is made of plastic and placed at an angle of 33°. Control and STZ-injected mice or  $db/db$  mice were placed individually in the central entry zone and allowed to

freely explore the apparatus for 5 min while being videotaped. The total number of arm entries and alterations between the arms are recorded. Frequent exploration in all three arms indicates normal spontaneous exploration, whereas restricted arm entries indicate deficits in spontaneous exploration. Alternations were defined as successive entries into each of the three arms as on overlapping triplet sets (ABC, BCA, ...). Percent of spontaneous alternation was defined as the ratio of actual (total alternations) to possible (total arm entries - 2) number of alternations  $\times 100$ . Alternate arm returns (AARs) and same arm returns (SARs) were also scored for each animal in order to assess aspects of attention within spontaneous working memory [23]. Total entries were scored as an index of ambulatory activity in the Y maze. Mice showing scores below six entries were excluded. A global analysis of data was made using ANOVA with the Dunnett's test post hoc comparisons, whereas comparisons between two groups for individual time points were done using the unpaired Student's *t* test.

### Morris Water Maze

The Morris water maze (MWM) was first established by neuroscientist Richard G. Morris in 1981 in order to test hippocampal-dependent learning, including acquisition of spatial memory and long-term spatial memory [24]. The theory behind it is that the animal must learn to use local cues to navigate the shortest path to the hidden platform when started from different, random locations around the perimeter of the water tank. Most protocols use four start locations: N, S, E, and W. Animals are given a series of daily trials using a semi-random set of start locations. Semi-random start position sets are most common, such that the four positions are used, with the restriction that one trial each day is from each of the four positions. Mice were randomly selected to control ( $n = 8$ ) and STZ groups ( $n = 20$ ). The MWM test was performed 12 weeks after STZ injections. On the first day of MWM test, each mouse was allowed to swim freely in water for 2 min where the platform had been removed, observing the swim action and speed of the mouse in order to eliminate unqualified animals. On the next day, each rodent was discharged into the water with a platform placed inside from a marked starting point in one of the four quadrants, facing the tank wall, encompassing training for 3 days. Mice were assessed in the probe trial 24 h after the last training session that consisted of a 60-s free swim in the pool without the platform. Each animal's performance was monitored using the Any-Maze™ Video Tracking System (Stoelting Co., Wood Dale, IL), which provided data for the acquisition parameters (latency to find the platform and distance swam) and the probe-trial parameter (number of entries to the target platform zone and time in quadrants). For the better assessment of learning ability of the mouse, a statistical analysis was made of the latency to find the platform and the number of repeated entries after first entry.

### In Vivo Permeability Assay

Changes in BBB permeability were assessed using the fluorescent tracer, sodium-fluorescein (Na-F) as described [25, 26]. Briefly, to prevent blood clotting in the vessels, animals were injected ip with heparin (20 U) followed intravenous (iv) injection of 50  $\mu$ L of 2% sodium fluorescein (NaF) in PBS. The tracer was allowed to circulate for 30 min. The mice were anesthetized and then transcardially perfused with PBS until colorless perfusion was visualized. The animals were then decapitated and the brains quickly isolated. After removal of the olfactory bulbs, cerebellum, and brain stem, the tissue was weighed and homogenized in 10 times volume of 50% trichloroacetic acid. The homogenate was centrifuged for 10 min at 13,000 $\times$ g and the supernatant was neutralized with 5 M NaOH (1:0.8). The amount of Na-F was measured using a Synergy 2 plate reader (BioTek, Winooski, VT). Fluorescent dye content was calculated using external standards; data are expressed as amount of tracer per mg of tissue.

### Mouse Brain Tissues

Microscopic examination of the brains used a standardized protocol with sections from the neocortex (frontal and parietal), basal ganglia, hippocampus, midbrain, pons, medulla, and cerebellum. Paraffin sections (5  $\mu$ m) were stained with hematoxylin-eosin. One section from the frontal cortical lobe was used for the evaluation of neuroinflammation and BBB structure by immunohistochemistry using the following antibodies: IBA (1:100; Wako Chemicals USA, Richmond, VA) for microglial activation, claudin-5 (1:50; Thermo Fisher Scientific, Waltham, MA) for endothelial cells, occludin (1:50; Novus Biologicals, Littleton, CO), and CD13 for pericytes (1:1000; R&D Systems, Minneapolis, MN). Primary antibodies were detected by Dako Envision Kit (Dako, Carpinteria, CA) or Vectastain Elite Kit (Vector Laboratories, Burlingame, CA) with either DAB (single stain) or Vector Red substrate (for double stains). Samples were imaged under  $\times 20$  objective magnification using a DS-Fi1c camera (Nikon Corporation, Tokyo) configured to an upright microscope (i80 Eclipse, Nikon). Immunostains for CD13/Iba1 were assessed in blinded fashion using a semi-quantitative scoring protocol: 0—negative staining, 1—mild positivity (< 10% of cells), 2—moderate positivity (10–75%), and 3—strong positivity (75%) [27]. CD13 assessment was limited to capillaries (no more than 6  $\mu$ m in diameter). For each animal, four to six randomly selected fields in the cortex were analyzed. Immunostains for claudin-5 and occludin were evaluated in blinded fashion using semi-quantitative scoring: 0—no staining; 1—weak staining (< 10% of capillaries); 2—moderate, variable labeling (10–75% capillaries); 3—strong, variable staining (> 75% capillaries); and 4—strong, uniform staining (95%).

## Brain Microvessel Isolation

Mouse brain microvessels (BMVs) were isolated using a modified protocol based on previously published studies [25, 28, 29]. In short, mice were overdosed with CO<sub>2</sub> and their brains harvested. All following steps were carried out on ice (or at 4 °C). Following a wash in phosphate-buffered saline, the brains were homogenized using a dounce homogenizer (0.25-mm clearance) (whole brain is defined as the S0 fraction; the nomenclature of S0, S1, and S5 describes the BMV fractionation steps consistent with the BMV isolation procedure as described below and previously by Yousif [29]). Overall, 15 mL of 30% Ficoll was added to 10 mL of the homogenate and mixed thoroughly. The resulting density gradient was centrifuged at 5800×g for 20 min (the pellet is defined as S1 fraction). The pellet was resuspended in 1 mL phosphate-buffered saline with 1% bovine serum albumin and passed through a glass bead column, with 100-µm nylon mesh filter on the top and a 40-µm nylon mesh filter at the bottom. The glass beads were gently agitated in phosphate-buffered saline with 1% bovine serum albumin to obtain BMVs. The resulting sample was washed with bovine serum albumin-free phosphate-buffered saline before use in experiments and is defined as the S5 fraction.

## PCR Array and qPCR

Total RNA was extracted from FFPE paraffin-embedded (FFPE) cortical tissues (same area as for IHC) using RecoverAll™ Total Nucleic Acid Isolation Kit [30–33] and from BMVs using PARIS™ RNA Isolation Kit (both Thermo Fisher Scientific). Total RNA (200 ng) was converted to complementary DNA (cDNA) using RT<sup>2</sup> PreAMP cDNA Synthesis Kit (Qiagen, Hilden, Germany). A PCR-based microarray assay for evaluating the expression of genes involved in inflammatory response and autoimmunity used RT<sup>2</sup>-profiler PCR Array (PAMM-077Z) and endothelial cell biology RT<sup>2</sup>-profiler PCR Array (PAMM-015Z) (SA Biosciences Corp., Frederick, MD) [26]. Profiling was performed for cDNA from two separate experiments. Data were scrutinized using a web-based analysis tool (SA Biosciences/Qiagen). Specific primers and probes for LTα, CD40lg, Myd88, and SLC2A1 (Glut1) genes were obtained from Thermo Fisher Scientific, and analyses were executed using the StepOnePlus real-time PCR system (Thermo Fisher Scientific). Amplification was examined using the ΔΔCt method, using a web-based data investigation tool (SABiosciences/Qiagen) by normalization to housekeeping genes and fold change calculated from the difference between experimental condition and untreated control. Fold changes of <2 or >2 were considered significant. Data are presented from two independent experiments, and each group is comprised of three to four individual mice. To eliminate biased data, two people performed analysis in blinded fashion.

Pathway analysis was performed by commercially available Ingenuity® Pathway Analysis (IPA®) system tools (Qiagen Bioinformatics, Redwood City, CA).

## Soluble Receptor for AGE Detection

Soluble receptor for AGEs (sRAGE) was measured in mouse serum utilizing a commercially available ELISA Kit (R&D Systems, Minneapolis, MN), according to the manufacturer's instructions. Data are presented as triplicates for each mouse and groups were comprised of 3–14 individual mice.

## Statistical Analysis

Results are expressed as the mean ± SEM of experiments conducted multiple times. Multiple group comparisons were performed by one-way analysis of variance with Dunnett's post hoc tests. Statistical analyses were performed utilizing Prism v5 software (GraphPad Software Inc., La Jolla, CA). Differences were considered significant at *p* values < 0.05.

## Results

### High Blood Glucose Is Associated With Memory Impairment in Both Type 1 and Type 2 DM Models

A summary of body weights and glucose readings is provided in Table 1. C57-STZ-treated mice displayed a 3-fold increase in fasting BGL and a significant decrease in body weight, mimicking body weight decline in humans with diabetes type 1 [34]. Db/db mice presented much higher BGL, 4.9- and 1.35-fold vs. C57-STZ-treated mice, respectively. Db/db mice also showed significant obese phenotype, being 1.55-fold heavier than their heterozygous counterparts, characteristic of DM type 2 patients [35].

In order to evaluate cognitive function in DM models, we used two well-established tests, Y maze and MWM. The Y maze spontaneous alternation paradigm is based on the ordinary tendency of rodents to explore a novel environment [23]. When positioned in the Y maze, mice will explore the least

**Table 1** Body mass and blood glucose levels in mice

Group/treatment	Body weight (g)	Glucose levels (mg/ml)
NT	28.06 ± 2.08	105.7 ± 21.54
STZ	24.42 ± 1.5*	365.78 ± 138.42**
db/hemi	30.71 ± 0.53	137.13 ± 6.95
db/db	43.99 ± 2.28**	491.91 ± 27.11***

\**p* < 0.05, \*\**p* < 0.01, or \*\*\**p* < 0.001 indicate significance vs. control (NT for STZ-treated group, and db/hemi for db/db mice)

recently visited arm, and thus tend to alternate visits between the three arms. An animal with an impaired working memory cannot remember which arm it has just visited, and thus shows decreased spontaneous alternation [21–23]. In Y maze tests, mice treated with STZ (12 weeks prior to test) showed significant ( $p < 0.001$  vs. NT) reduction of  $17 \pm 4\%$  in alternations (Fig. 1a). Type 2 DM db/db mice featured even greater memory loss with a reduction of  $25 \pm 6.5\%$  ( $p < 0.001$  vs. hemizygous) (Fig. 1a). Regression analysis showed that there was strong correlation between high BGL and memory deficits (low percent in alternations) in STZ-treated wild-type (WT) C57BL/6 and db/db mice (Fig. 1b, c).

C57BL/6 mice (with or without STZ treatment) were also tested for spatial memory function using the MWM evaluating hippocampal-dependent learning, including acquisition of spatial memory and long-term spatial memory [24]. In these experiments, we performed visible platform training followed by hidden platform testing with four probe trials per day [24, 36, 37]. All mice in each group were able to reach the training criterion within 4 days and were similarly proficient swimmers. However, only mice with the highest BGL (400–500 mg/dL) showed significant ( $p = 0.007$ ) latency in time to reach the hidden platform for the first time on the test day (Fig. 2a) and longer distance traveled until first entry in the target zone (data not shown). Mice with BGL of 250–350 or 400–500 mg/dL presented significantly diminished memory as measured by the number of repeated entries to the hidden platform (Fig. 2b). Interestingly, within the group of mice with high BGL, there were mice that showed mild or worse memory phenotypes. We decided to assign labels to these subgroups as “semi-impaired” for mild or “impaired” for worse memory phenotype, respectively (Fig. 2). In total, these results confirm our hypothesis that high BGL are associated with memory loss.

### Increased BBB Permeability in DM Type 1 and 2 Models

We evaluated BBB permeability in animals with STZ-induced hyperglycemia using the fluorescent tracer, NaF, as described [26]. The amount of NaF in the cerebrum was elevated as compared to untreated controls, and regression analysis showed a correlation between permeability level and BGL with  $R^2 = 0.4428$  in STZ-treated mice (Fig. 3a, b). Similarly, we also found 2.2-fold increased BBB permeability in db/db mice as compared to heterozygous controls with normal BGL (Fig. 3c). Next, regression analysis revealed strong correlation between memory loss (measured by percent of alternations in Y maze) and permeability level with  $R^2 = 0.5689$  in STZ-treated mice and  $R^2 = 0.9460$  in db/db mice, with  $p = 0.0073$  and  $p = 0.0054$ , respectively (Fig. 3d, e).

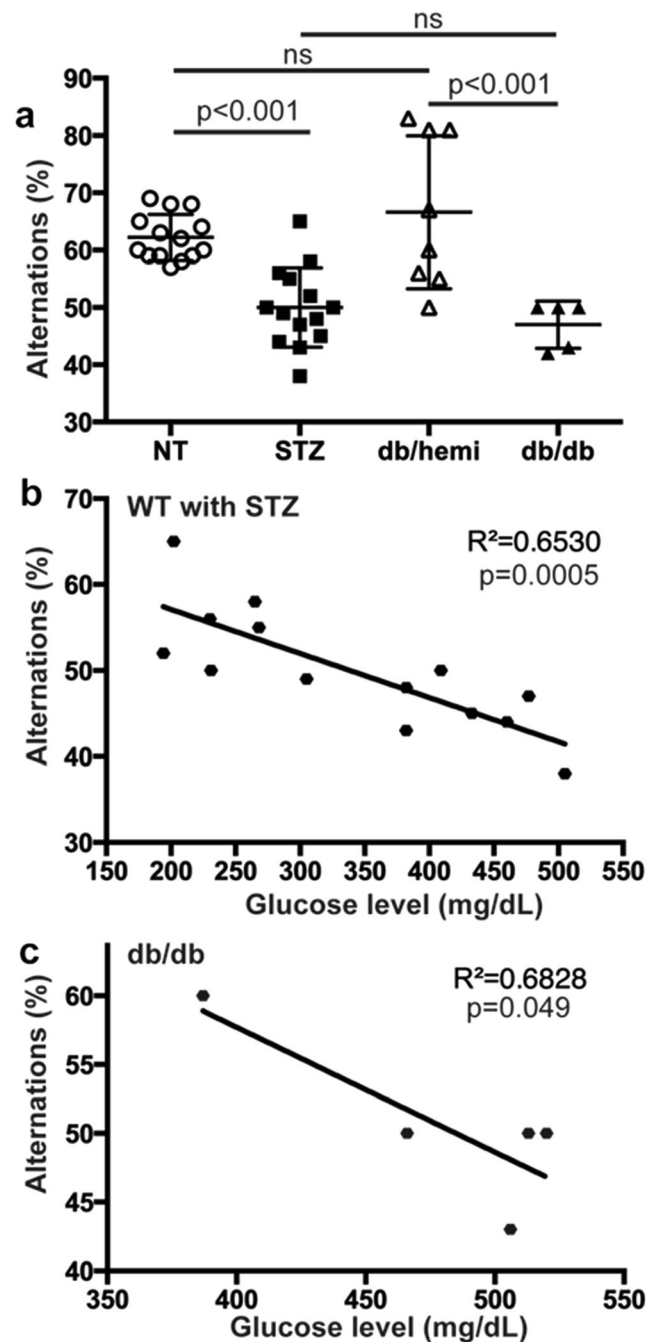


**Fig. 1** High glucose levels lead to memory deficits in types 1 and 2 diabetes mice. **a** Percentage of alternations measured by Y maze test in type 1 DM (STZ-treated or non-treated mice) or type 2 DM (db/db or heterozygous db/hemi) mice. Regression analysis of percent of alternations vs. glucose levels in WT mice, with or without STZ-induced diabetes (**b**) or in db/db mice (**c**).  $p$  values indicate significance between NT control ( $n = 14$ ) and STZ-treated animals ( $n = 14$ ), db/db mice ( $n = 5$ ), or db/hemi mice ( $n = 8$ )

### Diabetes Causes Inflammation in Brain BMVs

It has been suggested that sRAGE serve as decoys for AGEs, thus reducing RAGE signaling and inflammation [38–41]. We evaluated sRAGE levels in serum of DM type 1 and 2 mice

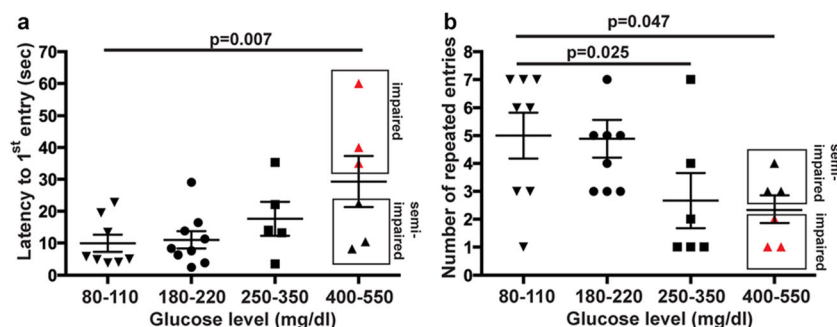


**Fig. 2** High glucose levels diminish memory in type 1 diabetes mice. Morris water maze results are presented as time to reach (latency) the target platform zone for non-treated (BGL = 80–110 mg/dl) and STZ-treated mice with different glucose levels (a) and the number of

repeated entries to the target platform zone for STZ-treated mice with different glucose levels (b). Results are shown as mean  $\pm$  SEM (six to nine animals per group). *p* values indicated on figures indicate significance vs. non-treated (BGL = 80–110 mg/dl)

using commercially available ELISA and discovered that DM mice had significantly  $\sim$ 1.4–1.6-fold lower levels of sRAGE than their control counterparts (Fig. 3f), suggesting a higher potential for inflammation in DM mice. The state of systemic inflammation that impairs endothelial function and contributes to atherosclerosis has been associated with DM [42]. DM patients are believed to acquire endothelial pathological phenotype due to the high levels of circulating inflammatory markers, including tumor necrosis factor- $\alpha$  (TNF $\alpha$ ), C-reactive protein, interleukin-6 (IL-6), and intercellular adhesion molecule 1 (ICAM-1) [43–47]. To evaluate relevant molecule expression in brain endothelium of diabetic mice, we

isolated BMVs and profiled the expression of genes commonly involved in regulation of endothelial functions and inflammation. Utilizing a commercially available qPCR-based array, 84 genes were analyzed. All gene expression data were then analyzed by IPA<sup>®</sup> system tools. Fifty-four genes related to pathways regulating angiogenesis, inflammation, vasoconstriction/vasodilation, and platelet activation were deregulated by at least 2-fold. Since we found differences in memory phenotypes (Fig. 2), we explored whether there would be any dissimilarity between semi-impaired and impaired mice in deregulated gene expression. Indeed, many genes had significant fold-change differences between these two groups

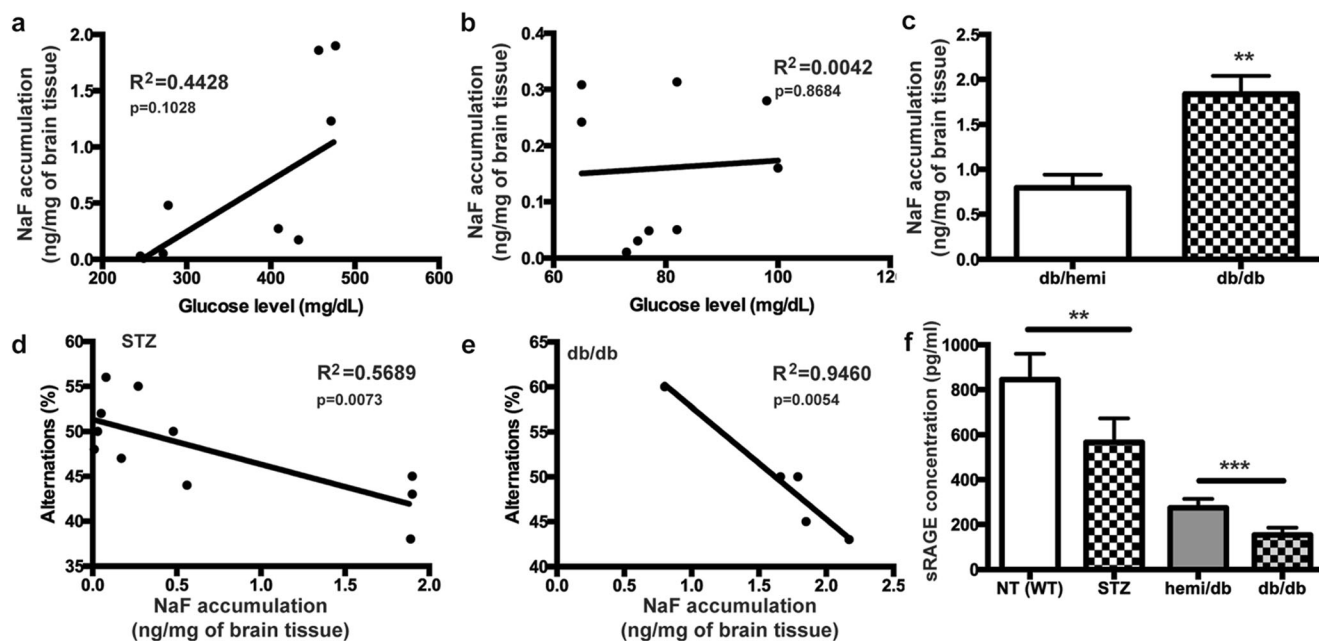


**Fig. 3** Hyperglycemia-driven BBB permeability triggers memory loss in DM mice. Regression analysis of permeability (measured by NaF accumulation in the brain) vs. glucose levels in mice with (a) or without (b) STZ-induced diabetes. c Enhanced BBB permeability in db/db mice (measured by NaF accumulation in the brain). Regression analysis of memory loss (alternation percent) vs. permeability (measured by NaF accumulation in the brain) in WT mice with STZ-

induced (DM type 1) (d) or db/db (DM type 2) (e). f Decreased levels of sRAGE measured by ELISA. \*\**p* < 0.05 or \*\*\**p* < 0.01 vs. control [untreated (NT) control (*n* = 14), STZ-treated animals (*n* = 14), db/db mice (*n* = 5), or db/hemi mice (*n* = 5)]. Results for both permeability and sRAGE are presented as the mean  $\pm$  SEM from triplicate serum samples

(Fig. 4a). Among them were eNOS, TNF $\alpha$ , TGF $\beta$ 1, Tymp, and MMP9 that have been shown to affect microvessel functions [48–53]. Next, we wanted to see if genes that were significantly upregulated in mice with impaired memory would be affected in BMVs isolated from db/db mice. qPCR analysis revealed that many of the genes upregulated in STZ-treated

mice with memory deficits also showed enhanced expression in BMVs from db/db mice, some of these genes to a much greater extent (Fig. 4b).

Other genes upregulated in brain BMVs included several chemokines promoting monocyte and lymphocyte attraction (CCL2, CCL5, CXCL2, CXCL3), adhesion molecules

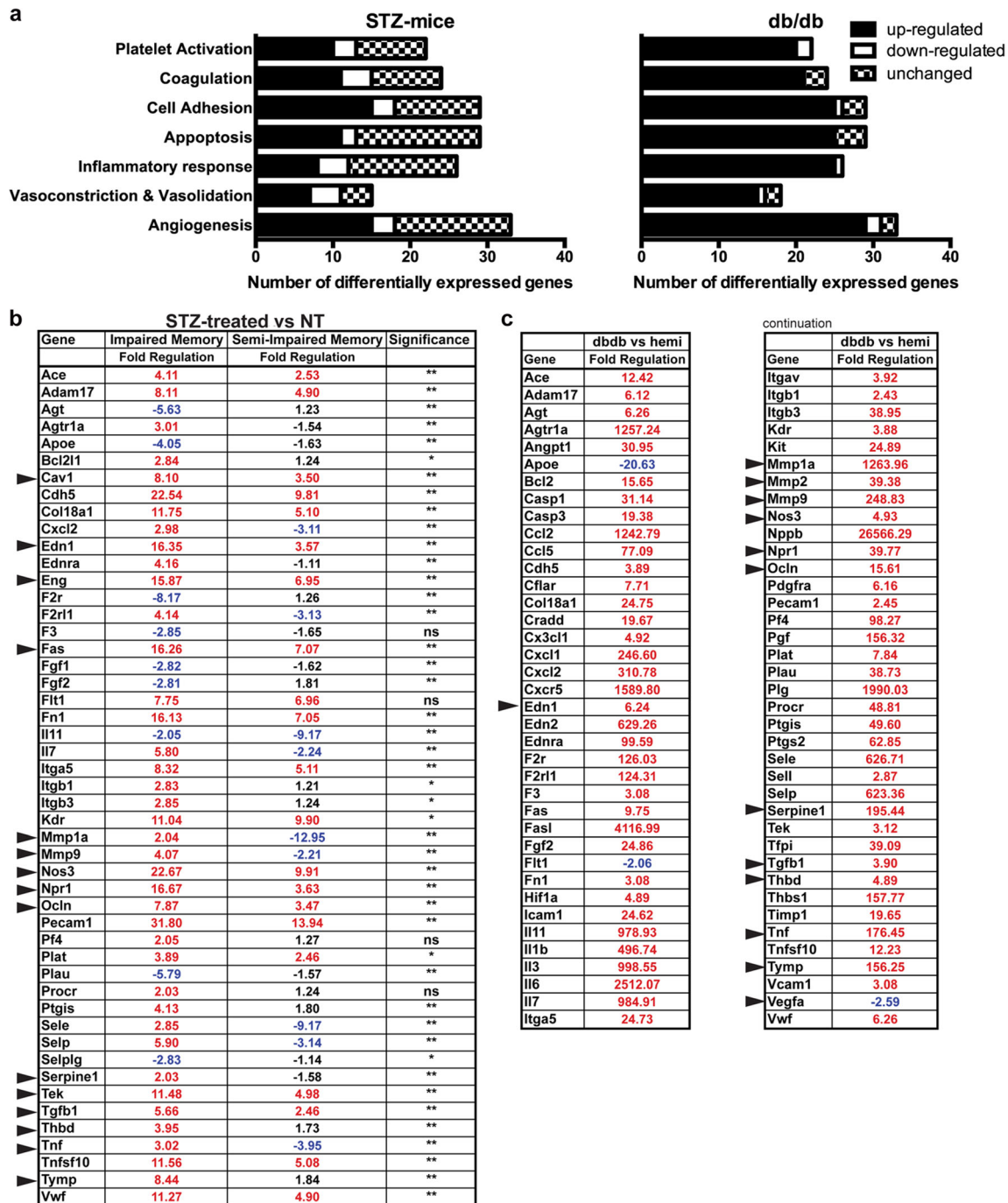


**Fig. 4** High glucose levels cause inflammation in brain microvessels. qPCR analysis of inflammatory response array for mRNA extracted from microvessels isolated from STZ-treated or db/db mice or their controls. IPA® analysis of differentially expressed genes (a). Fold regulation of the genes in STZ-treated vs. NT control (b) or db/db mice

vs. hemizygous controls (c). ns indicates no significance, and \*\* $p < 0.01$  indicates significance between mice with impaired vs. semi-impaired memory. Arrows point to genes described in the literature to be involved in BBB permeability

facilitating leukocyte adhesion (Pecam1, E-selectin),  $\beta$ -integrins (mediating adhesion of endothelial cells to basement membranes), and prostaglandin synthase. Such changes in gene expression are overall indicative of a pro-inflammatory phenotype, which directly or indirectly (enhanced interactions with white blood cells) can contribute to enhanced BBB permeability in diabetic animals. Of interest is that some of these genes showed significantly higher expression in type 2 DM as compared to type 1 DM animals. Despite our assumption that the TJ protein, occludin, or adherent junction protein (AJ), cadherin 5, would be downregulated in DM animals with enhanced BBB permeability, we found 8–16- and 4–22-fold increases in expression of these TJ and AJ protein genes, suggesting improper folding or incorporation in the cell membrane that may reflect a compensatory phenomenon in DM.

### Signs of Neuroinflammation in DM Animal Models Parallel Loss of Pericyte Coverage and Decrease in TJ Protein Expression

To assess inflammatory status in the brain tissue, we performed expression profiling of the genes regulating inflammatory pathways. Messenger RNA (mRNA) was extracted from the cortex area in contralateral hemisphere from the same mice that were used for BMV gene profiling (Fig. 5). Many genes were significantly affected in STZ-treated mice (Fig. 5a). Two of these genes,  $LT\alpha$  (TNF $\beta$ ) and CD40lg, have been described in the literature to be upregulated in AD or other types of dementia [54–57], and Myd88 to be downregulated [58]. We evaluated expression of these genes in db/db mice and

found that  $LT\alpha$  and Myd88 had a similar regulation profile, while CD40lg did not change in db/db mice vs. controls (Fig. 5b). Glucose transporter, Glut1 (SLC2A1), gene has been shown to be upregulated in blood vessels in mice with diabetic retinopathy [59]. Therefore, we decided to assess Glut1 levels in microvessels isolated from diabetic mice; indeed, both DM model mice showed higher Glut1 gene expression than their control counterparts (Fig. 5c). Interestingly enough, we found that in STZ-treated mice, there was a wide distribution in fold changes in gene expression. When we matched the gene expression data with our Morris water maze data (Fig. 2), we found a significant difference in fold changes between mice that showed impaired (marked in red) or semi-impaired phenotypes ( $p < 0.05$ ) (Fig. 5c).

Immunohistochemical evaluation of the cortex showed  $1.50 \pm 0.09$ -fold increase in ICAM-1 expression in STZ-treated mice vs. non-treated mice (Fig. 6a–h), whereas db/db mice displayed  $2.00 \pm 0.13$ -fold increase in ICAM-1 expression (Fig. 6d–h).

Next, we evaluated microglial reaction (Iba1), pericyte coverage (CD13), and TJ (claudin-5) in type 1 and type 2 DM mice models, STZ-diabetic mice, and db/db mice by immunohistochemistry. We found that STZ-diabetic mice showed a significant decrease in pericyte presence at the BBB and enhanced microglial reaction in diabetic mice as compared to controls with normal BGL (Fig. 7a, c). Similar immunohistochemical assessment of db/db mice displayed enhanced microglial reaction and diminished pericyte coverage in diabetic vs. control animals (Fig. 7b, d). Then, we appraised expression of the TJ proteins in the cortex area

**Fig. 5** Hyperglycemia causes inflammation in brain tissue and increased Glut1 expression in microvessels. qPCR analysis of an inflammatory response array for mRNA extracted from brain tissue isolated from STZ-treated or non-treated WT mice (a). qPCR data for  $LT\alpha$ , Myd88, and CD40lg in brains of db/db mice (b). qPCR data for Glut1 gene in cerebral microvessels in DM types 1 and 2 mouse models (c). qPCR was done in triplicate and results are shown as mean  $\pm$  SEM (three animals per group). ns indicates no significance, and \* $p < 0.05$  or \*\* $p < 0.01$  indicates significance between diabetic mice and their respective controls. # $p < 0.05$  indicates significance between mice with impaired vs. semi-impaired memory

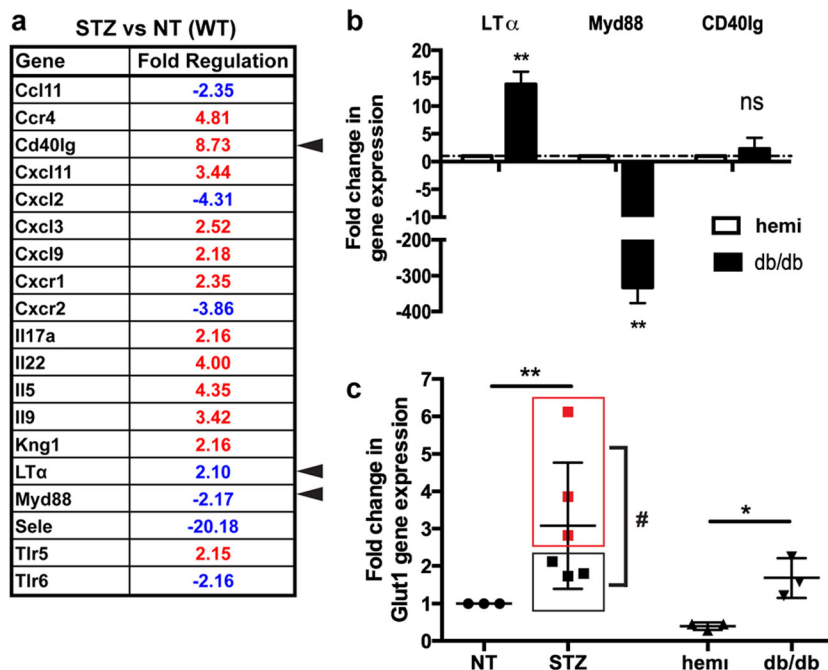
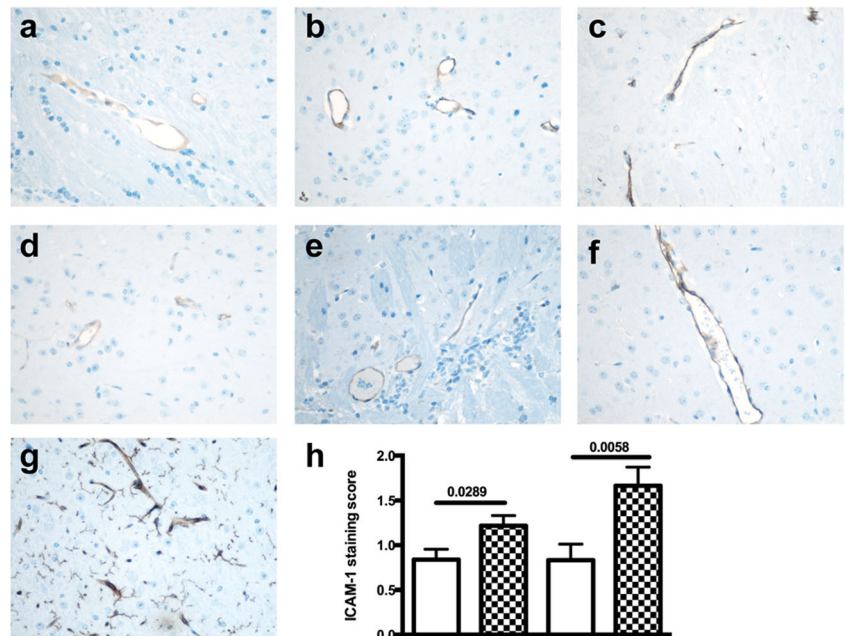


**Fig. 6** Enhanced expression of ICAM-1 in brain endothelium in DM types 1 and 2 mouse models. **a–c** Brain microvascular endothelial cells showed increased staining for ICAM-1 (**b, c**) in STZ-treated vs. control untreated mice (**a**). **d–f** Db/db homozygous mice (when compared to control heterozygous animals) (**d**) demonstrated enhanced expression of ICAM-1 in endothelial cells of capillaries and venules (**e, f**). **g** LPS-injected mouse used as a positive control demonstrated very high levels of ICAM-1 expression [60]. Original magnification, **a–g**  $\times 400$ . **h** Semi-quantitative evaluation of ICAM-1 staining was performed as described [27].  $**p < 0.002$



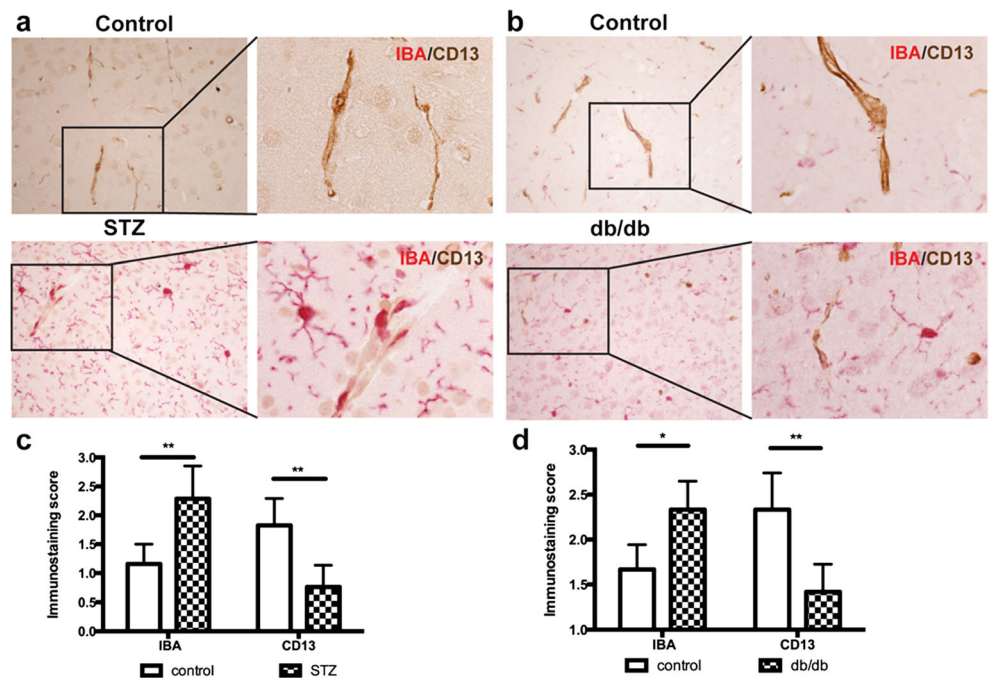
and found a significant decrease in claudin-5 expression in both DM models:  $16.2 \pm 5.4\%$  decrease in STZ-treated mice (Fig. 8a, c) and  $33.7 \pm 6.6\%$  in db/db mice (Fig. 8b, d). Evaluation of occludin expression on serial sections showed  $28.8 \pm 8.6\%$  diminution in the STZ diabetic model and  $51 \pm 4.5\%$  decrease in db/db mice when compared to respective controls (Fig. 8e, f).

Taken together, our results suggest a causative link between BBB dysfunction and cognitive deterioration in diabetic conditions.

## Discussion

Cerebrovascular pathology is often found in a wide variety of cognitive impairment or dementia disorders. One of the indicators of cerebral vascular disease is BBB dysfunction [61, 62]. The BBB serves as a selective diffusion barrier at the level of the cerebral microvascular endothelium to maintain homeostasis in the CNS by regulating ion balance, aiding in nutritional transport, and blocking influx of potentially neurotoxic molecules from the circulation [61, 62]. DM is a

**Fig. 7** Microglial activation and decreased pericyte coverage of the BBB in DM type 1 and 2 models. Enhanced microglial staining (Iba1, red) was associated with diminished pericyte coverage (CD13, brown) in STZ-treated (**a**) or db/db (**b**) vs. respective control mice. Original magnification was  $\times 400$ , and  $\times 1000$  in marked areas. **c, d** Semi-quantitative evaluation of double Iba1/CD13 staining was performed as described [27].  $*p < 0.05$ ,  $**p < 0.002$  represent significance vs. control



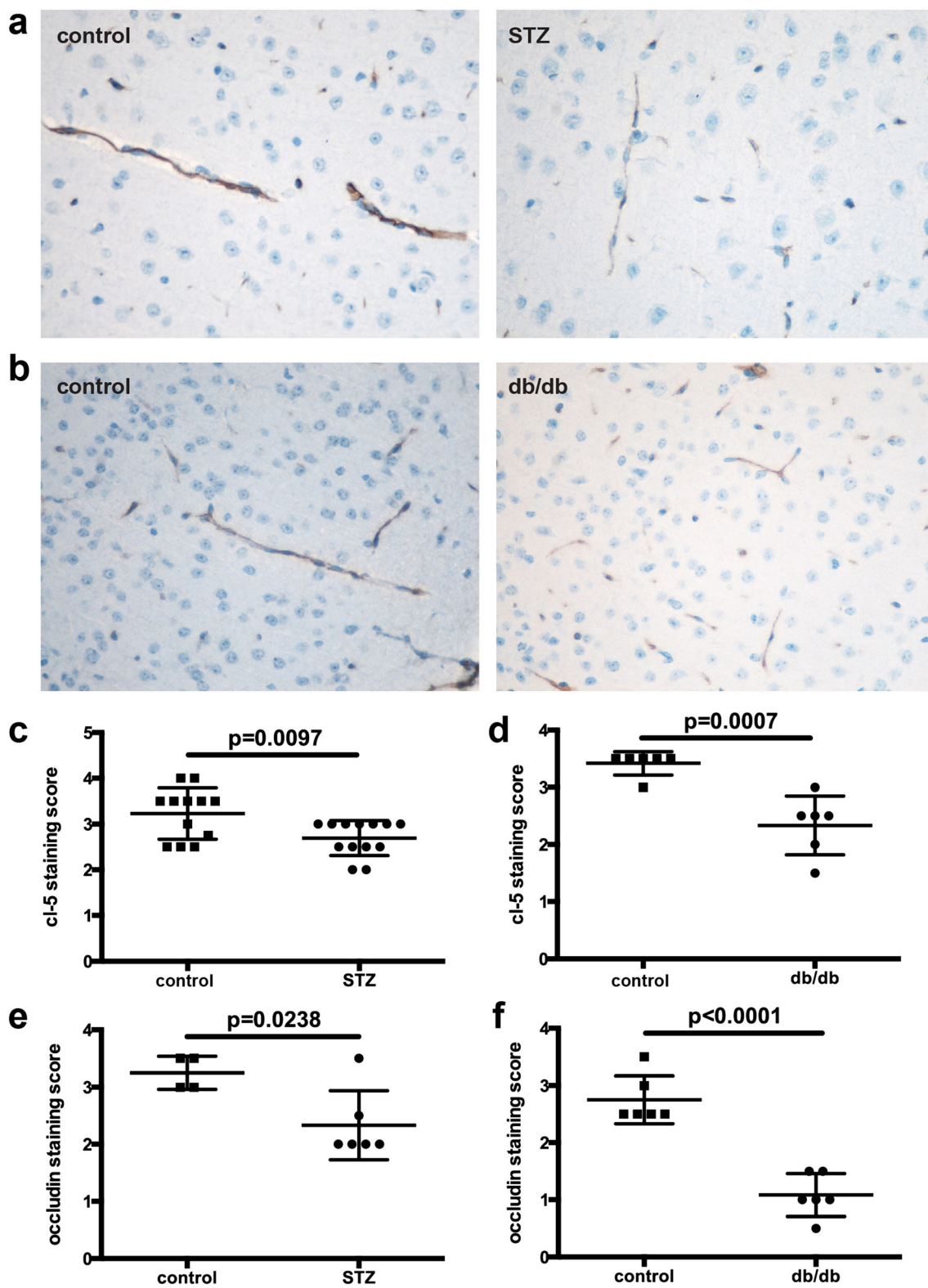


**Fig. 8** Claudin-5 and occludin protein expression is decreased in BMVs in DM type 1 and 2 models. Claudin-5 immunostaining is diminished (cl-5, brown) in STZ-treated (a) or db/db (b) vs. respective control mice.

Original magnification was  $\times 400$ . Semi-quantitative evaluation of claudin-5 (c, d) and occludin (e, f) staining was performed as described [27]

metabolic disorder characterized by hyperglycemia leading to end-organ injury in various organs due to microvascular

compromise (cardiovascular disease, nephropathy, and retinopathy) and inflammation. Learning abilities and memory

deficits have been documented in DM type 1 or type 2 patients [3–5], which might be due to cerebral vascular dysfunction. Association between microvascular changes and cognitive decline in DM has not been substantiated until very recently, with defects noted in blood perfusion, neuronal function, white matter microstructure, and metabolic function [7, 63].

BBB breakdown has been suggested as one of the causes of dementia in DM and AD [64]. However, the exact mechanisms of injury, relationship between enhanced permeability and memory loss, differences between DM types 1 and 2, and therapeutic potential of BBB protective strategies in cognitive decline are currently unknown. Here, we investigated the idea that DM types 1 and 2 decrease BBB integrity directly (via effects on brain endothelium and pericytes) and promote a pro-inflammatory phenotype of brain endothelium (resulting in a low-level inflammation) that further exacerbates barrier injury. We used animal models of DM types 1 and 2 and found that both models mice displayed a significant increase in BGL vs. control counterparts, mimicking hyperglycemia in DM patients [34, 35]. DM mice exhibited memory decline, confirmed by two well-established tests, Y maze and MWM [23, 24]. DM mice showed deterioration in their abilities in acquisition and long-term spatial memory similar to recent study [65]. STZ-injected mice displayed a broad range of BGL, but only mice with the highest BGL showed significant latency in spatial memory acquisition (time to reach hidden platform for the first time) and to memorize platform location (number of repeated entries). Mice that showed mild or worse memory phenotypes (marked as semi-impaired or impaired, respectively) demonstrated significantly different gene profiling in BMVs isolated from these animals. Among deregulated genes, there were many genes involved in inflammation and barrier destabilizing molecules (MMP9, eNOS, TGF $\beta$ , TNF $\alpha$ , Tymp) [48–53]. Several studies have suggested that sRAGE serves as a decoy for AGEs, thus reducing RAGE signaling and inflammation [38–41]. We discovered that DM mice had significantly lower levels of sRAGE than control animals, suggestive of a higher potential for inflammation in DM mice.

We showed increased BBB permeability in DM type 1 and 2 animals that was significantly associated with hyperglycemia and memory deficits. These changes paralleled deregulation of genes in brain endothelium associated with BBB injury and inflammation. In spite of our assumption that in DM animals with enhanced BBB permeability, TJ protein occludin or AJ protein cadherin 5 would be downregulated, we found their levels highly increased, implying improper folding or incorporation in cell membranes that may reflect a compensatory phenomenon in DM. Interestingly, we found significant reduction in TJ expression (protein) by immunohistochemistry (occludin and claudin-5) in both DM animal models as compared to controls (Fig. 8). Similarly, Li et al. demonstrated a decrease in the amount of occludin detected by western

blotting of isolated CNS microvessels in STZ-diabetic mice [66]. They also admitted that post-translational oxidative modifications or phosphorylation might be responsible for increased barrier permeability [67]. Differences might be explained as due to mRNA vs. protein detection for TJ proteins associated with adaptive mechanism, and further studies are needed to clarify this phenomenon.

Gene profiling resulted in significant upregulation of pro-inflammatory pathways in the brain tissues of the DM mice, which resulted in microglial activation, reduced pericyte coverage, shown by immunohistochemical assessment. Salameh et al. recently showed pericyte loss in STZ-induced diabetic mouse brains [68]. Pericytes are essential for the viability and function of the blood-retinal barrier and BBB [10, 68–70] and their loss, which is caused by hyperglycemia-induced oxidative damage, is associated with diseases such as diabetic retinopathy and Alzheimer's disease [71, 72]. Mice in both DM types displayed a significant decrease in TJ protein (claudin-5) expression. Takechi et al. recently showed that in a high-fat and high-fructose diet-induced DM model, reduction in expression of TJ proteins, occludin and ZO-1, was also associated with increased BBB leakiness, astrogliosis, neuroinflammation, and memory loss (as shown by MWM latency) [73]. Immunohistochemical evaluation showed significant increase in ICAM-1 expression in DM mice. DM patients are believed to acquire endothelial pathological phenotype due to the high levels of circulating inflammatory markers and ICAM-1 [44, 73]. Previously, diminution in pericyte presence has been described in DM both in the blood-retinal barrier and BBB [74]. Pericytes provide functional support to the brain endothelium and their loss leads to enhanced permeability and tissue injury in DM [75] and neuroinflammatory conditions [61]. Of interest, DM retinopathy is a predictor of decline, presumably due to CNS microvasculature demise [76]. All these factors together might explain the abnormal BBB permeability observed in DM mice.

We found several pro-inflammatory genes to be upregulated in DM type 1 animals, including chemokines. Among deregulated genes, we identified a few genes known to be associated with cognitive deficit; LT $\alpha$  (TNF $\beta$ ) and CD40lg were found to be upregulated [54–57] in AD or other type of dementia, and Myd88 to be downregulated [58]. Recently, the Glut1 gene has been shown to be upregulated in blood vessels in mice with diabetic retinopathy [59]. Recent studies recognized diabetic retinopathy to be one of the prognosticators for mental decline [76]. Our results showed that mice with the highest Glut1 levels were the mice with memory deficits. Glut1 is also critical for the maintenance of appropriate brain capillary networks, cerebral blood flow, and BBB integrity, as demonstrated in humans with SLC2A1 mutations and Slc2a1 transgenic mice, which contributes to neurodegeneration and behavioral deficits in a murine model of AD and GLUT1 deficiency [77–79]. Targeting Glut1 in diabetes might provide

future therapeutic directions in alleviating retinopathy or memory deficits.

The current study presents a strong association between hyperglycemia, BBB permeability, and cognitive dysfunction in both DM type animal models. Hyperglycemic animals showed a pro-inflammatory phenotype both in BMVs and brain tissue. Disruption of the BBB was associated with and present in animals with cognitive decline, similar to recently demonstrated BBB dysfunction association with cognitive decline in DM patients [11], and was associated with increased levels of vascular dysfunction markers in CSF. Ample work remains to be done regarding the understanding of mechanisms of BBB changes and its involvement in dementia development in DM, and is of high significance due to the potential of employing novel therapeutic interventions protecting BBB and preventing cognitive impairment.

**Acknowledgments** This work was supported in part by NIH research grants AA015913 (YP), MH1106967 (YP), MH65151 (YP), MH115786 (YP), and NS101135 (SR). The authors express their grateful acknowledgement for proofreading and editing to Nancy L. Reichenbach.

**Authors' Contributions** VZR, SG, AS, MW, NAH, MAK, YVB, and AKS—data acquisition and analysis, drafting, revising, and final approval article. SR and YP—conception and design, data acquisition, analysis and interpretation, drafting and revising article, and final approval.

## Compliance with Ethical Standards

**Conflict of Interest** The authors declare that they have no conflict of interest.

## References

- Snyder EL, Stramer SL, Benjamin RJ (2015) The safety of the blood supply—time to raise the bar. *N Engl J Med* 373(9):882. <https://doi.org/10.1056/NEJMc1507761>
- Kisler K, Nelson AR, Rege SV, Ramanathan A, Wang Y, Ahuja A, Lazic D, Tsai PS et al (2017) Pericyte degeneration leads to neurovascular uncoupling and limits oxygen supply to brain. *Nat Neurosci* 20(3):406–416. <https://doi.org/10.1038/nn.4489>
- Moran C, Tapp RJ, Hughes AD, Magnussen CG, Blizzard L, Phan TG, Beare R, Witt N et al (2016) The Association of Type 2 diabetes mellitus with cerebral gray matter volume is independent of retinal vascular architecture and retinopathy. *J Diabetes Res* 2016: 6328953–6328959. <https://doi.org/10.1155/2016/6328953>
- Prasad S, Sajja RK, Naik P, Cucullo L (2014) Diabetes mellitus and blood-brain barrier dysfunction: An overview. *Aust J Pharm* 2(2): 125. <https://doi.org/10.4172/2329-6887.1000125>
- Sutherland GT, Lim J, Srikanth V, Bruce DG (2017) Epidemiological approaches to understanding the link between type 2 diabetes and dementia. *J Alzheimers Dis* 59(2):393–403. <https://doi.org/10.3233/jad-161194>
- Di Marco E, Jha JC, Sharma A, Wilkinson-Berka JL, Jandeleit-Dahm KA, de Haan JB (2015) are reactive oxygen species still the basis for diabetic complications? *Clin Sci (London, England: 1979)* 129(2):199–216. <https://doi.org/10.1042/cs20150093>
- van Bussel FCG, Backes WH, Hofman PAM, van Oostenbrugge RJ, van Boxtel MPJ, Verhey FRJ, Steinbusch HWM, Schram MT et al (2017) Cerebral pathology and cognition in diabetes: The merits of multiparametric neuroimaging. *Front Neurosci* 11:188. <https://doi.org/10.3389/fnins.2017.00188>
- Imamine R, Kawamura T, Umemura T, Umegaki H, Kawano N, Hotta M, Kouchi Y, Hatsuda S et al (2011) Does cerebral small vessel disease predict future decline of cognitive function in elderly people with type 2 diabetes? *Diabetes Res Clin Pract* 94(1):91–99. <https://doi.org/10.1016/j.diabres.2011.06.014>
- Bogush M, Heldt NA, Persidsky Y (2017) Blood brain barrier injury in diabetes: Unrecognized effects on brain and cognition. *J NeuroImmune Pharmacol* 12:593–601. <https://doi.org/10.1007/s11481-017-9752-7>
- Hill J, Rom S, Ramirez SH, Persidsky Y (2014) Emerging roles of Pericytes in the regulation of the neurovascular unit in health and disease. *J NeuroImmune Pharmacol* 9(5):591–605. <https://doi.org/10.1007/s11481-014-9557-x>
- Janelidze S, Hertz J, Nagga K, Nilsson K, Nilsson C, Wennstrom M, van Westen D, Blennow K et al (2017) Increased blood-brain barrier permeability is associated with dementia and diabetes but not amyloid pathology or APOE genotype. *Neurobiol Aging* 51: 104–112. <https://doi.org/10.1016/j.neurobiolaging.2016.11.017>
- Sharma B, Singh N (2010) Pitavastatin and 4'-hydroxy-3'-methoxyacetophenone (HMAP) reduce cognitive dysfunction in vascular dementia during experimental diabetes. *Curr Neurovasc Res* 7(3):180–191
- Stranahan AM, Hao S, Dey A, Yu X, Baban B (2016) Blood-brain barrier breakdown promotes macrophage infiltration and cognitive impairment in leptin receptor-deficient mice. *J Cereb Blood Flow Metab* 36(12):2108–2121. <https://doi.org/10.1177/0271678x16642233>
- Brownlee M (2001) Biochemistry and molecular cell biology of diabetic complications. *Nature* 414(6865):813–820. <https://doi.org/10.1038/414813a>
- Dias IH, Griffiths HR (2014) Oxidative stress in diabetes - circulating advanced glycation end products, lipid oxidation and vascular disease. *Ann Clin Biochem* 51(Pt 2):125–127. <https://doi.org/10.1177/0004563213508747>
- Lu QY, Chen W, Lu L, Zheng Z, Xu X (2014) Involvement of RhoA/ROCK1 signaling pathway in hyperglycemia-induced microvascular endothelial dysfunction in diabetic retinopathy. *Int J Clin Exp Pathol* 7(10):7268–7277
- Cukierman-Yaffe T, Gerstein HC, Williamson JD, Lazar RM, Lovato L, Miller ME, Coker LH, Murray A et al (2009) Relationship between baseline glycemic control and cognitive function in individuals with type 2 diabetes and other cardiovascular risk factors: The action to control cardiovascular risk in diabetes-memory in diabetes (ACCORD-MIND) trial. *Diabetes Care* 32(2): 221–226. <https://doi.org/10.2337/dc08-1153>
- Umegaki H (2014) Type 2 diabetes as a risk factor for cognitive impairment: Current insights. *Clin Interv Aging* 9:1011–1019. <https://doi.org/10.2147/cia.s48926>
- Whitmer RA, Karter AJ, Yaffe K, Quesenberry CP Jr, Selby JV (2009) Hypoglycemic episodes and risk of dementia in older patients with type 2 diabetes mellitus. *JAMA* 301(15):1565–1572. <https://doi.org/10.1001/jama.2009.460>
- McEvoy RC, Andersson J, Sandler S, Hellerstrom C (1984) Multiple low-dose streptozotocin-induced diabetes in the mouse. Evidence for stimulation of a cytotoxic cellular immune response against an insulin-producing beta cell line. *J Clin Invest* 74(3):715–722. <https://doi.org/10.1172/JCII11487>
- Holcomb LA, Gordon MN, Jantzen P, Hsiao K, Duff K, Morgan D (1999) Behavioral changes in transgenic mice expressing both amyloid precursor protein and presenilin-1 mutations: Lack of association with amyloid deposits. *Behav Genet* 29(3):177–185

22. Wall PM, Messier C (2002) Infralimbic kappa opioid and muscarinic M1 receptor interactions in the concurrent modulation of anxiety and memory. *Psychopharmacology* 160(3):233–244. <https://doi.org/10.1007/s00213-001-0979-9>
23. Wietrzyk M, Meziane H, Sutter A, Ghyselinc N, Chapman PF, Chambon P, Krezel W (2005) Working memory deficits in retinoid X receptor gamma-deficient mice. *Learn Mem* 12(3):318–326. <https://doi.org/10.1101/lm.89805>
24. Morris RGM (1981) Spatial localization does not require the presence of local cues. *Learn Motiv* 12:239–260
25. Rom S, Dykstra H, Zuluaga-Ramirez V, Reichenbach NL, Persidsky Y (2015) miR-98 and let-7g\* protect the blood-brain barrier under neuroinflammatory conditions. *J Cereb Blood Flow Metab* 35:1957–1965. <https://doi.org/10.1038/jcbfm.2015.154>
26. Rom S, Zuluaga-Ramirez V, Dykstra H, Reichenbach N, Ramirez SH, Persidsky Y (2015) Poly(ADP-ribose) polymerase-1 inhibition in brain endothelium protects the blood–brain barrier under physiologic and neuroinflammatory conditions. *J Cereb Blood Flow Metab* 35(1):28–36. <https://doi.org/10.1038/jcbfm.2014.167>
27. Persidsky Y, Hill J, Zhang M, Dykstra H, Winfield M, Reichenbach NL, Potula R, Mukherjee A et al (2016) Dysfunction of brain pericytes in chronic neuroinflammation. *J Cereb Blood Flow Metab* 36(4):794–807. <https://doi.org/10.1177/0271678X15606149>
28. Hartz AM, Notenboom S, Bauer B (2009) Signaling to P-glycoprotein—a new therapeutic target to treat drug-resistant epilepsy? *Drug News Perspect* 22(7):393–397. <https://doi.org/10.1358/dnp.2009.22.7.1401354>
29. Yousif S, Marie-Claire C, Roux F, Scherrmann JM, Decleves X (2007) Expression of drug transporters at the blood-brain barrier using an optimized isolated rat brain microvessel strategy. *Brain Res* 1134(1):1–11. <https://doi.org/10.1016/j.brainres.2006.11.089>
30. Gouveia GR, Ferreira SC, Ferreira JE, Siqueira SA, Pereira J (2014) Comparison of two methods of RNA extraction from formalin-fixed paraffin-embedded tissue specimens. *Biomed Res Int* 2014:151724–151725. <https://doi.org/10.1155/2014/151724>
31. Kotorashvili A, Ramnauth A, Liu C, Lin J, Ye K, Kim R, Hazan R, Rohan T et al (2012) Effective DNA/RNA co-extraction for analysis of microRNAs, mRNAs, and genomic DNA from formalin-fixed paraffin-embedded specimens. *PLoS One* 7(4):e34683. <https://doi.org/10.1371/journal.pone.0034683>
32. Landolt L, Marti HP, Beisland C, Flatberg A, Eikrem OS (2016) RNA extraction for RNA sequencing of archival renal tissues. *Scand J Clin Lab Invest* 76(5):426–434. <https://doi.org/10.1080/00365513.2016.1177660>
33. Okello JB, Zurek J, Devault AM, Kuch M, Okwi AL, Sewankambo NK, Bimenya GS, Poinar D et al (2010) Comparison of methods in the recovery of nucleic acids from archival formalin-fixed paraffin-embedded autopsy tissues. *Anal Biochem* 400(1):110–117. <https://doi.org/10.1016/j.ab.2010.01.014>
34. Gao H, Zhao Q, Song Z, Yang Z, Wu Y, Tang S, Alahdal M, Zhang Y et al (2017) PGLP-1, a novel long-acting dual-function GLP-1 analog, ameliorates streptozotocin-induced hyperglycemia and inhibits body weight loss. *FASEB J* 31:3527–3539. <https://doi.org/10.1096/fj.201700002R>
35. Burguera B, Ali KF, Brito JP (2017) Antiobesity drugs in the management of type 2 diabetes: A shift in thinking? *Cleve Clin J Med* 84(7 Suppl 1):S39–s46. <https://doi.org/10.3949/ccjm.84.s1.05>
36. Bromley-Brits K, Deng Y, Song W (2011) Morris water maze test for learning and memory deficits in Alzheimer's disease model mice. *J Vis Exp* 53. <https://doi.org/10.3791/2920>
37. Eichenbaum H, Stewart C, Morris RG (1990) Hippocampal representation in place learning. *J Neurosci* 10(11):3531–3542
38. Arabi YM, Dehbi M, Rishu AH, Baturcam E, Kahoul SH, Brits RJ, Naidu B, Bouchama A (2011) sRAGE in diabetic and non-diabetic critically ill patients: Effects of intensive insulin therapy. *Crit Care* 15(4):R203. <https://doi.org/10.1186/cc10420>
39. Devangelio E, Santilli F, Formoso G, Ferroni P, Bucciarelli L, Michetti N, Clissa C, Ciabattini G et al (2007) Soluble RAGE in type 2 diabetes: Association with oxidative stress. *Free Radic Biol Med* 43(4):511–518. <https://doi.org/10.1016/j.freeradbiomed.2007.03.015>
40. Heier M, Margeisdottir HD, Gaarder M, Stensaeth KH, Brunborg C, Torjesen PA, Seljeflot I, Hanssen KF et al (2015) Soluble RAGE and atherosclerosis in youth with type 1 diabetes: A 5-year follow-up study. *Cardiovasc Diabetol* 14:126. <https://doi.org/10.1186/s12933-015-0292-2>
41. Hanford LE, Enghild JJ, Valnickova Z, Petersen SV, Schaefer LM, Schaefer TM, Reinhart TA, Oury TD (2004) Purification and characterization of mouse soluble receptor for advanced glycation end products (sRAGE). *J Biol Chem* 279(48):50019–50024. <https://doi.org/10.1074/jbc.M409782200>
42. Beckman JA, Creager MA, Libby P (2002) Diabetes and atherosclerosis: Epidemiology, pathophysiology, and management. *JAMA* 287(19):2570–2581
43. Keane JF Jr, Larson MG, Vasani RS, Wilson PW, Lipinska I, Corey D, Massaro JM, Sutherland P et al (2003) Obesity and systemic oxidative stress: Clinical correlates of oxidative stress in the Framingham study. *Arterioscler Thromb Vasc Biol* 23(3):434–439. <https://doi.org/10.1161/01.ATV.0000058402.34138.11>
44. Keane JF Jr, Massaro JM, Larson MG, Vasani RS, Wilson PW, Lipinska I, Corey D, Sutherland P et al (2004) Heritability and correlates of intercellular adhesion molecule-1 in the Framingham offspring study. *J Am Coll Cardiol* 44(1):168–173. <https://doi.org/10.1016/j.jacc.2004.03.048>
45. Schulze MB, Rimm EB, Li T, Rifai N, Stampfer MJ, Hu FB (2004) C-reactive protein and incident cardiovascular events among men with diabetes. *Diabetes Care* 27(4):889–894
46. Stocker R, Keane JF Jr (2005) New insights on oxidative stress in the artery wall. *J Thromb Haemost* 3(8):1825–1834. <https://doi.org/10.1111/j.1538-7836.2005.01370.x>
47. Vozarova B, Weyer C, Hanson K, Tataranni PA, Bogardus C, Pratley RE (2001) Circulating interleukin-6 in relation to adiposity, insulin action, and insulin secretion. *Obes Res* 9(7):414–417. <https://doi.org/10.1038/oby.2001.54>
48. Wong D, Dorovini-Zis K, Vincent SR (2004) Cytokines, nitric oxide, and cGMP modulate the permeability of an in vitro model of the human blood-brain barrier. *Exp Neurol* 190(2):446–455. <https://doi.org/10.1016/j.expneurol.2004.08.008>
49. Nwariaku FE, Rothenbach P, Liu Z, Zhu X, Turnage RH, Terada LS (2003) Rho inhibition decreases TNF-induced endothelial MAPK activation and monolayer permeability. *J Appl Physiol* 95(5):1889–1895
50. Wright JL, Merchant RE (1994) Blood-brain barrier changes following intracerebral injection of human recombinant tumor necrosis factor-alpha in the rat. *J Neuro-Oncol* 20(1):17–25
51. Chapouly C, Tadesse Argaw A, Homg S, Castro K, Zhang J, Asp L, Loo H, Laitman BM et al (2015) Astrocytic TYMP and VEGFA drive blood-brain barrier opening in inflammatory central nervous system lesions. *Brain* 138(Pt 6):1548–1567. <https://doi.org/10.1093/brain/awv077>
52. Mailankody S, Dangeti GV, Soundravally R, Joseph NM, Mandal J, Dutta TK, Kadiravan T (2017) Cerebrospinal fluid matrix metalloproteinase 9 levels, blood-brain barrier permeability, and treatment outcome in tuberculous meningitis. *PLoS One* 12(7):e0181262. <https://doi.org/10.1371/journal.pone.0181262>
53. McMillin MA, Frampton GA, Seiwel AP, Patel NS, Jacobs AN, DeMorrow S (2015) TGFbeta1 exacerbates blood-brain barrier permeability in a mouse model of hepatic encephalopathy via upregulation of MMP9 and downregulation of claudin-5. *Lab Invest* 95(8):903–913. <https://doi.org/10.1038/labinvest.2015.70>
54. Gemma C, Smith EM, Hughes TK Jr, Opp MR (2000) Human immunodeficiency virus glycoprotein 160 induces cytokine

- mRNA expression in the rat central nervous system. *Cell Mol Neurobiol* 20(4):419–431
55. Giunta B, Figueroa KP, Town T, Tan J (2009) Soluble CD40 ligand in dementia. *Drugs Future* 34(4):333–340. <https://doi.org/10.1358/dof.2009.034.04.1358595>
  56. Davidson DC, Hirschman MP, Sun A, Singh MV, Kasischke K, Maggirwar SB (2012) Excess soluble CD40L contributes to blood brain barrier permeability in vivo: Implications for HIV-associated neurocognitive disorders. *PLoS One* 7(12):e51793. <https://doi.org/10.1371/journal.pone.0051793>
  57. Yu S, Liu YP, Liu YH, Jiao SS, Liu L, Wang YJ, Fu WL (2016) Diagnostic utility of VEGF and soluble CD40L levels in serum of Alzheimer's patients. *Clin Chim Acta* 453:154–159. <https://doi.org/10.1016/j.cca.2015.12.018>
  58. Michaud JP, Richard KL, Rivest S (2011) MyD88-adaptor protein acts as a preventive mechanism for memory deficits in a mouse model of Alzheimer's disease. *Mol Neurodegener* 6(1):5. <https://doi.org/10.1186/1750-1326-6-5>
  59. Lu L, Seidel CP, Iwase T, Stevens RK, Gong YY, Wang X, Hackett SF, Campochiaro PA (2013) Suppression of GLUT1; a new strategy to prevent diabetic complications. *J Cell Physiol* 228(2):251–257. <https://doi.org/10.1002/jcp.24133>
  60. Ramirez SH, Hasko J, Skuba A, Fan S, Dykstra H, McCormick R, Reichenbach N, Krizbai I et al (2012) Activation of cannabinoid receptor 2 attenuates leukocyte-endothelial cell interactions and blood-brain barrier dysfunction under inflammatory conditions. *J Neurosci* 32(12):4004–4016. <https://doi.org/10.1523/JNEUROSCI.4628-11.2012>
  61. Zlokovic BV (2008) The blood-brain barrier in health and chronic neurodegenerative disorders. *Neuron* 57(2):178–201. <https://doi.org/10.1016/j.neuron.2008.01.003>
  62. Zlokovic BV (2010) Neurodegeneration and the neurovascular unit. *Nat Med* 16(12):1370–1371. <https://doi.org/10.1038/nm1210-1370>
  63. Cui Y, Liang X, Gu H, Hu Y, Zhao Z, Yang XY, Qian C, Yang Y et al (2017) Cerebral perfusion alterations in type 2 diabetes and its relation to insulin resistance and cognitive dysfunction. *Brain Imaging Behav* 11(5):1248–1257. <https://doi.org/10.1007/s11682-016-9583-9>
  64. Goldwaser EL, Acharya NK, Sarkar A, Godsey G, Nagele RG (2016) Breakdown of the Cerebrovasculature and blood-brain barrier: A mechanistic link between diabetes mellitus and Alzheimer's disease. *J Alzheimers Dis* 54(2):445–456. <https://doi.org/10.3233/jad-160284>
  65. Oliveira WH, Nunes AK, Franca ME, Santos LA, Los DB, Rocha SW, Barbosa KP, Rodrigues GB et al (2016) Effects of metformin on inflammation and short-term memory in streptozotocin-induced diabetic mice. *Brain Res* 1644:149–160. <https://doi.org/10.1016/j.brainres.2016.05.013>
  66. Li W, Maloney RE, Aw TY (2015) High glucose, glucose fluctuation and carbonyl stress enhance brain microvascular endothelial barrier dysfunction: Implications for diabetic cerebral microvasculature. *Redox Biol* 5:80–90. <https://doi.org/10.1016/j.redox.2015.03.005>
  67. Murakami T, Felinski EA, Antonetti DA (2009) Occludin phosphorylation and ubiquitination regulate tight junction trafficking and vascular endothelial growth factor-induced permeability. *J Biol Chem* 284(31):21036–21046. <https://doi.org/10.1074/jbc.M109.016766>
  68. Salameh TS, Shah GN, Price TO, Hayden MR, Banks WA (2016) Blood-brain barrier disruption and neurovascular unit dysfunction in diabetic mice: Protection with the mitochondrial carbonic anhydrase inhibitor Topiramate. *J Pharmacol Exp Ther* 359(3):452–459. <https://doi.org/10.1124/jpet.116.237057>
  69. Daneman R, Zhou L, Kebede AA, Barres BA (2010) Pericytes are required for blood-brain barrier integrity during embryogenesis. *Nature* 468(7323):562–566. <https://doi.org/10.1038/nature09513>
  70. Persidsky Y, Ramirez SH, Haorah J, Kanmogne GD (2006) Blood-brain barrier: Structural components and function under physiologic and pathologic conditions. *J NeuroImmune Pharmacol* 1(3):223–236. <https://doi.org/10.1007/s11481-006-9025-3>
  71. Hammes HP, Lin J, Renner O, Shani M, Lundqvist A, Betsholtz C, Brownlee M, Deutsch U (2002) Pericytes and the pathogenesis of diabetic retinopathy. *Diabetes* 51(10):3107–3112
  72. Sengillo JD, Winkler EA, Walker CT, Sullivan JS, Johnson M, Zlokovic BV (2013) Deficiency in mural vascular cells coincides with blood-brain barrier disruption in Alzheimer's disease. *Brain Pathol* 23(3):303–310. <https://doi.org/10.1111/bpa.12004>
  73. Takechi R, Lam V, Brook E, Giles C, Fimognari N, Mooranian A, Al-Salami H, Coulson SH et al (2017) Blood-brain barrier dysfunction precedes cognitive decline and neurodegeneration in diabetic insulin resistant mouse model: An implication for causal link. *Front Aging Neurosci* 9:399. <https://doi.org/10.3389/fnagi.2017.00399>
  74. Tien T, Muto T, Barrette K, Challyandra L, Roy S (2014) Downregulation of Connexin 43 promotes vascular cell loss and excess permeability associated with the development of vascular lesions in the diabetic retina. *Mol Vis* 20:732–741
  75. Shah GN, Morofuji Y, Banks WA, Price TO (2013) High glucose-induced mitochondrial respiration and reactive oxygen species in mouse cerebral pericytes is reversed by pharmacological inhibition of mitochondrial carbonic anhydrases: Implications for cerebral microvascular disease in diabetes. *Biochem Biophys Res Commun* 440(2):354–358. <https://doi.org/10.1016/j.bbrc.2013.09.086>
  76. Serlin Y, Shafat T, Levy J, Winter A, Shneck M, Knyazer B, Parnet Y, Shalev H et al (2016) Angiographic evidence of proliferative retinopathy predicts neuropsychiatric morbidity in diabetic patients. *Psychoneuroendocrinology* 67:163–170. <https://doi.org/10.1016/j.psyneuen.2016.02.009>
  77. Nelson AR, Sweeney MD, Sagare AP, Zlokovic BV (2016) Neurovascular dysfunction and neurodegeneration in dementia and Alzheimer's disease. *Biochim Biophys Acta* 1862(5):887–900. <https://doi.org/10.1016/j.bbdis.2015.12.016>
  78. Wang D, Kranz-Eble P, De Vivo DC (2000) Mutational analysis of GLUT1 (SLC2A1) in Glut-1 deficiency syndrome. *Hum Mutat* 16(3):224–231. [https://doi.org/10.1002/1098-1004\(200009\)16:3<224::AID-HUMU5>3.0.CO;2-P](https://doi.org/10.1002/1098-1004(200009)16:3<224::AID-HUMU5>3.0.CO;2-P)
  79. Winkler EA, Nishida Y, Sagare AP, Rege SV, Bell RD, Perlmutter D, Sengillo JD, Hillman S et al (2015) GLUT1 reductions exacerbate Alzheimer's disease vasculo-neuronal dysfunction and degeneration. *Nat Neurosci* 18(4):521–530. <https://doi.org/10.1038/nn.3966>